SIMULTANEOUS MEASUREMENT OF VELOCITY AND PARTICLE SIZE PROFILES WITH THE REFERENCE BEAM TECHNIQUE

M. Borys, V. Strunck, H. Müller, D. Dopheide

Physikalisch-Technische Bundesanstalt (PTB), Department 1.3 – Fluid Mechanics
D-38116 Braunschweig, Bundesallee 100, Germany
tel.: #49-531-592-1312, fax: #49-531-592-1305
e-mail: michael.borys@ptb.de

ABSTRACT

Laser Doppler velocity measurements based on the reference beam technique are well known since the initial work by Yeh and Cummins (1964). Due to the specific signal generation of a reference beam arrangement, a location of the trajectory of the scattering particle inside the measurement volume is possible by applying at least two receivers. Two alternative solutions to this problem with a spatial resolution of about 10 µm over a length of the measurement volume of more than 6 mm are described and experimentally verified in velocity profile measurements.

The application of the phase Doppler principle to the reference beam technique allows simultaneous measurement of velocity, size and position of each particle inside the measurement volume. With this reference beam PDA, the correlation between velocity, size and position of the disperse phase in multiphase flows with high velocity gradients can be investigated without a relative displacement of the optical set-up. The paper presents the theory of the reference beam PDA and first results of simultaneous measurements of velocity and particle size profiles in boundary layers. According to the results of theoretical and experimental investigations, the reference beam PDA is especially suited for particle sizing in the diameter range below 3 µm, i. e. a size range in which traditional phase Doppler systems suffer from a poor diameter resolution, and allows in extension of conventional phase Doppler systems a general improvement of the spatial and diameter resolution of phase Doppler measurements.

1. INTRODUCTION

The spatial resolution of conventional laser Doppler systems is limited by the dimensions of the measurement volume. In applications with high velocity gradients, e. g. measurements in boundary layers, the integration of the local velocity over the extension of the measurement volume of conventional laser Doppler systems cannot be neglected. Hence various methods have been developed in the past to improve the spatial resolution. These methods can be subdivided into methods of minimized intersection volumes of the laser beams (Karlson et al. 1992, Compton et al. 1996, Durst et al. 1996), selective spatial detection inside the measurement volume (Mazumder et al. 1981, Wei et al. 1989, Gusmeroli and Martinelli 1991, Wittig et al. 1996) or coincident measurements of multicomponent systems (Dopheide et al. 1993). All these methods apply a sequential velocity measurement at selected points to scan the part of the flow field of interest.

Similar difficulties occur with a simultaneous measurement of particle sizes based on the phase Doppler technique. Since velocity gradients and particle size distributions inside the measurement volume cannot be resolved with conventional phase Doppler systems, an investigation of particle size-dependent separation and migration effects required a displacement of the measurement volume relative to the measured object so far (Taniere et al. 1997, Chalé-Góngora and Brun 1998, Desantes et al. 1998).

2. FUNDAMENTALS

2.1 Location of the particle trajectory

The investigated configuration is based on a symmetric alignment of two laser Doppler systems according to the reference beam principle (receivers R_1 and R_2 in Fig. 1, Strunck et al. 1993). In contrast to the widely used "dual beam" or "differential Doppler" method, the Doppler signal is now generated by the superposition of a reference wave from the reference beam on the receiver and a wave scattered by a particle in the illuminating beam (Drain 1980). Each receiver has its own virtual measurement volume aligned along the axis of the respective illuminating beam. As a result of this symmetric structure, the angle between the main axes of these volumes corresponds to the beam crossing angle θ. From the Doppler frequency f_D of the received signals, the velocity v_x and thus the coordinate *z* of the particle trajectory can be determined as a function of the time shift Δt_{12} between the Doppler signals of the receivers R_1 and R_2

$$z(\Delta t_{12}) = \frac{v_x \Delta t_{12}}{2\tan(\theta/2)} \quad . \tag{1}$$

This measuring method was already successfully used for velocity measurements in laminar, transient and turbulent boundary layers (Strunck et al. 1994, 1998). Theoretical and experimental investigations have shown that a resolution in the order of magnitude of 10 µm over a length of about 6 mm in the *z*-direction can be achieved (Borys et al. 1998).

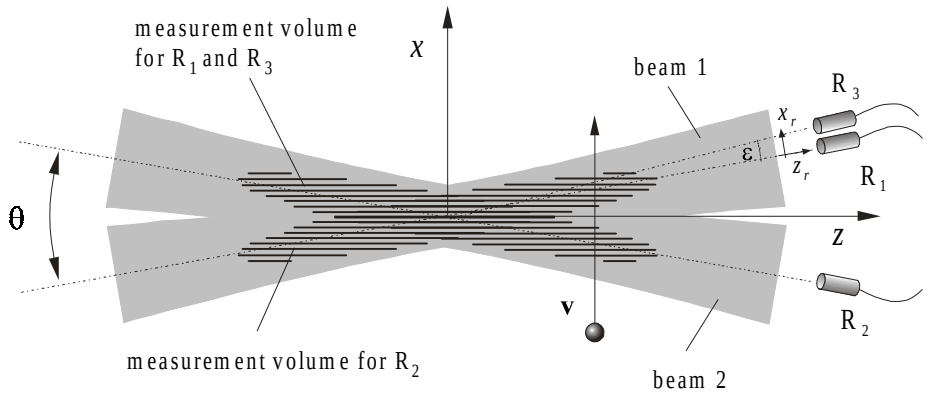

Fig. 1: Beam and receiver alignment of a reference beam PDA

An alternative method to locate the particle trajectory inside the measurement volume is based on the evaluation of the spatial frequency of the interference pattern in the reference beam. To describe the physical background of this method, we will consider the signal generation on the receiver R_1 in the following. For the receiver R_1 beam 1 is the reference beam and beam 2 the illuminating beam. The Doppler signal on R_1 is generated by superposition of the reference wave of beam 1 with the wave scattered by a particle in beam 2.

Depending on the position $z_2 = z / \cos(\theta/2)$ of the scattering particle along the axis of beam 2, reference and scattered wave include an angle

$$\alpha(z_2) = \arctan\left(\frac{z_2 \sin\theta}{r_{01} - z_2 \cos\theta}\right) \approx \frac{z_2 \sin\theta}{r_{01}} \tag{2}$$

with r_{01} as the distance of the receiver R_1 from the origin in the point of intersection of the laser beams. Figure 2 shows the interference of the reference beam with the scattered wave in the plane of receiver R_1 for two different angles α depending on the positions of the scattering particle along the beam axis of the illuminating beam z_2.

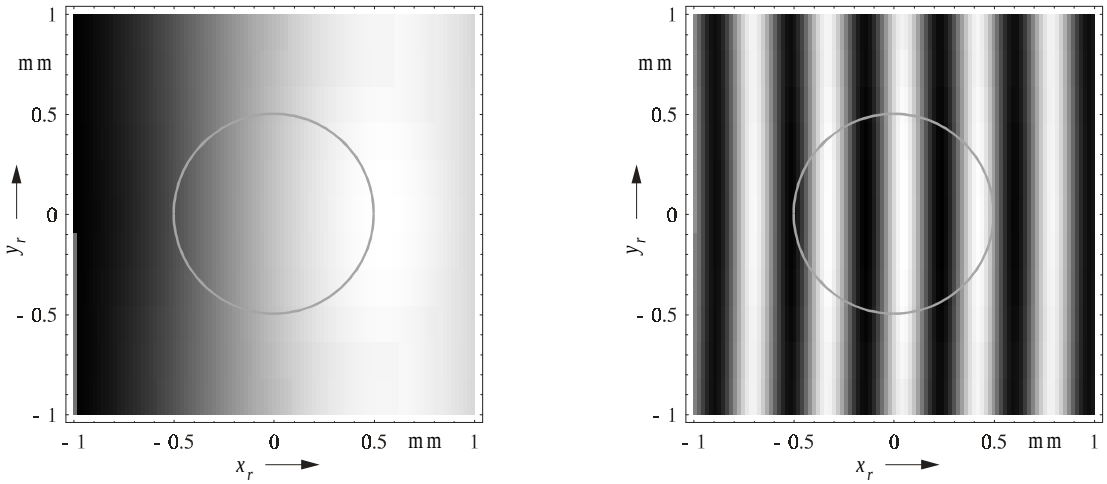

a) $z_2 = 1$ *mm* *b)* $z_2 = 10$ *mm*

Fig. 2: Interference of the reference beam with the scattered wave in the plane of receiver R_1 *for two different positions of the scattering particle along the beam axis of the illuminating beam* z_2 *(calculated by light scattering analysis according to the Fourier-Lorenz-Mie theory (FLMT, Albrecht et al. 1995), Parameters:* $\lambda = 852$ *nm,* $\theta = 9°$, $r_{01} = 0.7$ *m, radius of the beam waist* $r_b = 65$ *µm)*

The fringe spacing of the interference pattern in the receiver plane is given by

$$\Delta s(\alpha) = \frac{\lambda}{2\sin(\alpha/2)} \approx \frac{\lambda\, r_{01}}{z_2 \sin\theta} \ . \tag{3}$$

It should be noticed that due to the integration of the interference pattern over the receiver surface the visibility of the signal decreases with the fringe spacing $\Delta s(\alpha)$ and limits the range of constructive interference to (coherence cone, Drain 1980, Borys et al. 1998)

$$z_2 \le \frac{r_{01} \sin\alpha_c}{\sin(\theta + \alpha_c)} \tag{4}$$

with

$$\alpha_c = \arcsin\left(\frac{\lambda}{2 d_r}\right) \tag{5}$$

and the receiver diameter d_r.

Equation (3) allows a location of the particle trajectory inside the measurement volume based on an evaluation of the spatial frequency of the interference in the receiver plane of the reference beam. A realization of this principle is possible by a measurement of the spatial frequency over a detector line or matrix or by a simple measurement of the phase difference between the Doppler signals of at least two receivers in the reference beam. The latter is outlined in Fig. 1 by the receivers R_1 and R_3 in beam 1. These are displaced by $x_r = 2 r_{01} \sin(\varepsilon/2)$ in the receiver plane. From the phase difference $\Delta\Phi_{13}$ between the Doppler signals of the receivers the coordinate z_2 of the particle trajectory in the plane of the laser beams can be calculated according to

$$z_2 = \frac{r_{01}\sin\left(2\arcsin\left(\frac{\lambda\,\Delta\Phi_{13}}{4\pi\,x_r}\right)\right)}{\sin\left(\theta+2\arcsin\left(\frac{\lambda\,\Delta\Phi_{13}}{4\pi\,x_r}\right)\right)} \approx \frac{\lambda\,r_{01}}{2\pi\,x_r\sin(\theta)}\Delta\Phi_{13} \tag{6}$$

with a distance $r_{01} = r_{03}$ of the receivers R_1 and R_3 from the origin in the point of intersection of the laser beams. For phase differences $-\pi < \Delta\Phi_{13} < \pi$, the coordinate z_2 can be determined without ambiguity. Therefore the displacement between the receivers in the receiver plane x_r should be chosen as small as possible. The smallest value is reached if x_r is just the receiver diameter d_r with a phase range corresponding to the range of constructive interference over the receiver surface according to Eqs. (4) and (5). This value can be achieved in good approximation using integrated multi-element receivers or fiber arrangements. For an integrated receiver, for example CENTRONIC Ltd. type LD2-5T, with two elements with a diameter of $d_r = 500$ µm, a displacement of their centers in the *x*-direction of $x_r = 550$ µm, a receiver distance of $r_{0r} = 1$ m, a wavelength of $\lambda = 852$ nm and a beam crossing angle of $\theta = 9°$, particle trajectories can be located according to Eq. (6) without ambiguity in a range -5 mm< z_2 <5 mm. Whether the whole length corresponding to a phase difference of one period can be exploited depends on the signal quality and the lower bounds of the signal acquisition and validation. If a signal detection outside of this range cannot be excluded, ambiguities can be eliminated similar to the method used in the phase Doppler technique by additional receiver elements at positions displaced from the *x*-*z* plane and a distance $x_r < d_r$ from one receiver in the *x*-*z* plane. Because of the small angle $\varepsilon = 0.03°$ between the receivers in the example given above, the influence of the particle diameter on the measured phase difference can be neglected. The deviation of the measured Doppler frequencies is much smaller than 1% and can be easily corrected since the geometry is known.

2.2 Simultaneous particle sizing

A simultaneous measurement of particle sizes can be realized by an additional receiver pair outside of the laser beams. In this case, the particle sizes would be measured inside the measurement volume of a conventional phase Doppler system. This effort for extended hardware, signal acquisition and signal processing would not be necessary if in addition to the time shift the phase of the reference signals could be exploited. But in contrast to conventional phase Doppler systems, the Doppler signals are now generated due to the superposition of a reference wave from the reference beam on the receiver and a wave scattered by a particle in the illuminating beam instead of a superposition of two scattered waves. The physical background and characteristics of such a reference beam PDA will be described in a first step for particles in the vicinity of the point of intersection of the laser beams.

2.2.1 Phase difference of the reference signals in the range of geometrical optics

An analysis of the relations between the phase difference of the Doppler signals and the particle diameter in the considered reference system has to be performed similar to the known analysis of the "classical" PDA for reflection and refraction (Bachalo and Houser 1984, Bauckhage and Flögel 1984, Saffman et al. 1984). Because of the specifics of the reference beam technique, this will be described more detailed for the scattering orders reflection and 1st refraction.

Reflection

The alternating part of the Doppler signal is generated by the superposition of the field strength of the reference beam

$$\underline{E}_{b1} = E_{b1}(\mathbf{r}_{01})\cos(\omega t - \Phi_{b1}(\mathbf{r}_{01})) \tag{7}$$

and the wave scattered by the particle in the illuminating beam

$$\underline{E}_{s21} \sim E_{b2}(\mathbf{r}_{021})\cos(\omega t - \Phi_{021} - \mathbf{k}_{p21}\cdot\mathbf{r}_{p21}) \tag{8}$$

resulting in an intensity

$$I_{AC1} \sim E_{b1}(\mathbf{r}_{01})\,E_{b2}(\mathbf{r}_{021})\cos(\Phi_{b1}(\mathbf{r}_{01}) - \Phi_{021} - \mathbf{k}_{p21}\cdot\mathbf{r}_{p21}) \tag{9}$$

on the receiver R_1 in Fig. 3. The phase $\Phi_{b1}(\mathbf{r}_{01})$ describes the phase of the reference beam at the receiver position and Φ_{021} the phase of the illuminating beam at the interaction point $r_{r21}^{(1)}$ between the particle and the illuminating beam for reflection.

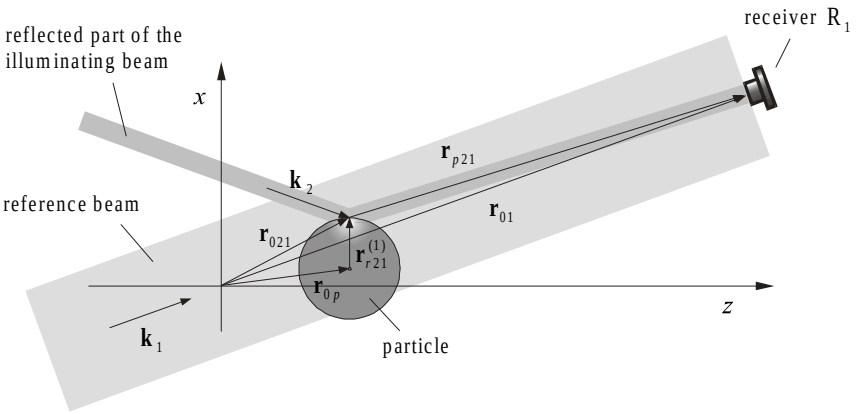

Fig. 3: Signal generation for the reference beam technique by reflection

For a Gaussian beam both can be described by

$$\Phi_b = k_b \left(x \sin(\pm\theta/2) + z\cos(\theta/2) + \frac{(x\cos(\theta/2) + z\sin(\pm\theta/2))^2 + y^2}{2R_b} \right) - \arctan\left(\frac{x\sin(\pm\theta/2) + z\cos(\theta/2)}{l_b} \right) \tag{10}$$

with the Rayleigh length l_b and the curvature of the wave front R_b (Albrecht 1986). The intensity on the receiver R_2 in Fig. 3 can be written in analogy to Eq. (9). From the phases of both intensities the phase difference is given by

$$\Delta\Phi_{12refl} = \Phi_1 - \Phi_2 = \Phi_{b1}(\mathbf{r}_{01}) + \Phi_{b2}(\mathbf{r}_{02}) - \Phi_{021} - \Phi_{012} - \mathbf{k}_{p21}\cdot\mathbf{r}_{p21} - \mathbf{k}_{p12}\cdot\mathbf{r}_{p12} \ . \tag{11}$$

This general formulation can be simplified for a receiver in the far field ($r_{01} >> r_{021}$), focused laser beams ($r_{01} >> l_b$) and a particle in the point of intersection of the beam axes ($r_{0p} = 0$) to

$$\Delta\Phi_{12refl} \approx \frac{2\pi}{\lambda}(\mathbf{e}_{01}\cdot\mathbf{r}^{(1)}_{r21} + \mathbf{e}_{02}\cdot\mathbf{r}^{(1)}_{r12} - \mathbf{e}_{k1}\cdot\mathbf{r}^{(1)}_{r12} - \mathbf{e}_{k2}\cdot\mathbf{r}^{(1)}_{r21}) - \pi \tag{12}$$

with $\mathbf{e}$ as the unit vector. Because of the symmetry of the used configuration we get

$$\mathbf{e}_{01}\cdot\mathbf{r}^{(1)}_{r21} = \mathbf{e}_{02}\cdot\mathbf{r}^{(1)}_{r12} = -\mathbf{e}_{k1}\cdot\mathbf{r}^{(1)}_{r12} = -\mathbf{e}_{k2}\cdot\mathbf{r}^{(1)}_{r21} = r_p\sin(\theta/2) \tag{13}$$

and

$$\Delta\Phi_{12refl} \approx \frac{2\pi}{\lambda} d_p 2\sin(\theta/2) - \pi = 2\pi\frac{d_p}{\Delta x} - \pi \tag{14}$$

with the particle diameter d_p and the fringe spacing of the virtual interference pattern Δx. This result can be simply interpreted by the glare points for reflection. Because of the symmetry of the used configuration, the distance between the glare points on the particle surface is just the particle diameter. Hence the relation between particle diameter and fringe spacing of the interference field gives the periods of the measured phase difference. Since the path difference between reference wave and reflected wave is equal to the difference between the waves reflected in the two beams, the particle size-dependent phase term in Eq. (14) is only a special case of the known phase Doppler relation for reflection (off-axis angle $\varphi = 0$, elevation angle $\psi = \pm\theta/2$). The additional phase shift by π results from the phase difference of $\pi/2$ between scattered wave and reference wave in the far field of a focused Gaussian beam ($r_{01} >> l_b$). It has to be canceled for a reference beam with a homogeneous field characteristic.

1st refraction

In addition to the described phase analysis for reflection, we have to consider for the 1st refraction the phase shift due to the path of the refracted light through the particle (Fig. 4). For the receivers R_1 and R_2 this additional phase can be described by

$$\mathbf{k}_{t21}\cdot\mathbf{r}_{t21}=\frac{2\pi}{\lambda}\left|\mathbf{r}_{r21}^{(2)}-\mathbf{r}_{r21}^{(1)}\right|=\frac{2\pi}{\lambda}m\,d_p\sin\tau'_{21}\quad\text{and}\quad\mathbf{k}_{t12}\cdot\mathbf{r}_{t12}=\frac{2\pi}{\lambda}\left|\mathbf{r}_{r12}^{(2)}-\mathbf{r}_{r12}^{(1)}\right|=\frac{2\pi}{\lambda}m\,d_p\sin\tau'_{12}\qquad(15)$$

respectively, with $m=n_{particle}/n_{continuum}$ as the relative refractive index. When extending Eq. (11) by these phase terms, we get

$$\Delta\Phi_{12refr}=\Phi_{b1}(\mathbf{r}_{01})+\Phi_{b2}(\mathbf{r}_{02})-\Phi_{021}-\Phi_{012}-\mathbf{k}_{t21}\cdot\mathbf{r}_{t21}-\mathbf{k}_{t12}\cdot\mathbf{r}_{t12}-\mathbf{k}_{p21}\cdot\mathbf{r}_{p21}-\mathbf{k}_{p12}\cdot\mathbf{r}_{p12}\ .\qquad(16)$$

Similar to the phase analysis for reflection this general formulation can be simplified for a receiver in the far field ($r_{01}>>r_{021}$), focused laser beams ($r_{01}>>l_b$) and a particle in the point of intersection of the beam axes ($r_{0p}=0$) to

$$\Delta\Phi_{12refr}\approx\frac{2\pi}{\lambda}\left\{\mathbf{e}_{01}\cdot\mathbf{r}_{r21}^{(2)}+\mathbf{e}_{02}\cdot\mathbf{r}_{r12}^{(2)}-\mathbf{e}_{k1}\cdot\mathbf{r}_{r12}^{(1)}-\mathbf{e}_{k2}\cdot\mathbf{r}_{r21}^{(1)}-m\,d_p(\sin\tau'_{21}+\sin\tau'_{12})\right\}-\pi\ .\qquad(17)$$

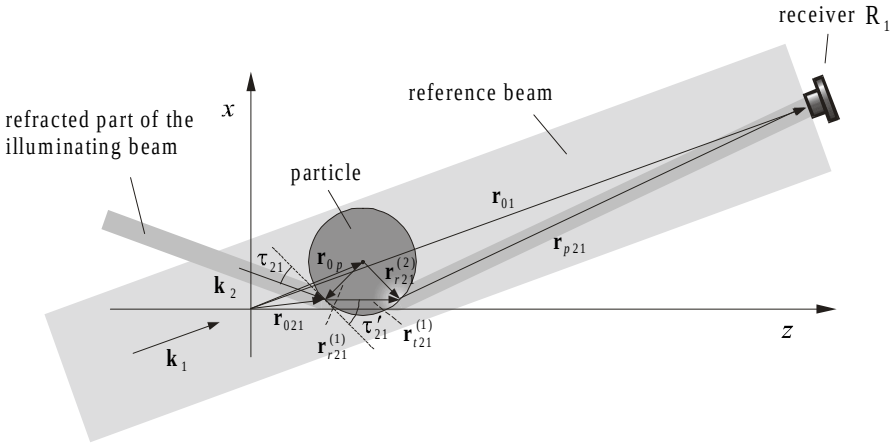

Fig. 4: Signal generation for the reference beam technique by refraction

Because of the symmetry of the used configuration, all phase terms in Eq. (17) can be expressed as a function of the wavelength λ, particle diameter d_p, relative refractive index m and intersection angle θ:

$$\Delta\Phi_{12refr}=-\frac{4\pi}{\lambda}d_p\sqrt{1+m^2-2m\cos(\theta/2)}-\pi\qquad(18)$$

For a small angle θ, the size-dependent phase difference of the reference beam PDA corresponds to twice the optical path difference between reference wave and refracted wave through the center of the particle ($\lim_{\theta\to0}\Delta\Phi_{12refr}=-(4\pi/\lambda)(m-1)\,d_p-\pi$). Under the same condition, the phase difference of a common PDA system for refraction

$$\Delta\Phi_{refr}=\frac{4\pi}{\lambda}d_p\left\{(m-1)-\sqrt{1+m^2-2m\cos(\theta/2)}\right\}\qquad(19)$$

would converge to zero. A comparison between the Eqs. (18) and (19) shows a much higher diameter resolution of the reference beam PDA (already mentioned by Strunck et al. 1994). Figure 5 gives the phase curves for a planar and a reference beam PDA. Although the angle between the receivers of the planar set-up was chosen larger, the diameter resolution of the reference PDA is more than five times higher. Hence a combination of a reference beam and a conventional PDA offers the possibility of improving the diameter resolution.

For transparent particles with diameters $d_p>>\lambda$, the influence of the refracted light dominates in the forward scattering direction. However, the superposition of diffracted and reflected light with the reference wave has to be taken into account. Similar to the known influence in conventional PDA systems, deviations from the linear phase diameter relationship have to be expected for the reference beam PDA. Figure 5 therefore shows a comparison between the phase diameter relation for the reference beam PDA according to Eq. (18) and the result of a light scattering analysis based on the Fourier-Lorenz-Mie theory (FLMT, Albrecht et al. 1995).

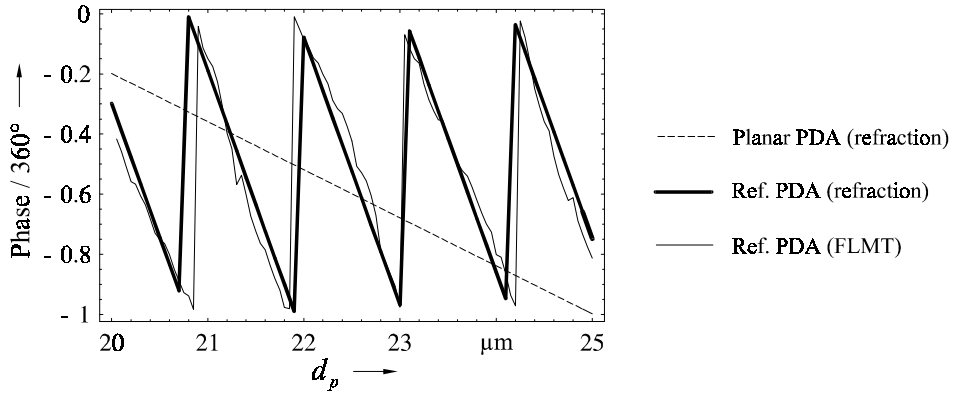

Fig. 5: Phase difference for refraction as a function of the particle diameter for a planar and reference beam PDA (Parameters: m=1.33, λ =852 nm, $\theta = 18.9°$, Planar PDA: $\psi = \pm 13°$)

2.2.2 Phase difference of the reference signals in the size range below 5 λ

Because of the poor diameter resolution, the scattered light power and strong oscillations in the phase diameter relation, common phase Doppler measurements are difficult in this size range. Figure 6 shows the phase difference as a function of the particle diameter for a standard, a planar and a reference beam PDA. In comparison to a common PDA, the curve of the reference beam PDA shows a behavior which is obviously different. Because of a phase difference of $\pi / 2$ between the phase of the reference wave in the far field of a focused Gaussian beam and a wave scattered by particles with diameters $d_p < \lambda / 5$, the phase difference in the Rayleigh region has a value of π instead of 0. In contrast to conventional PDA systems, the phase curve of the reference beam PDA has a more linear behavior and provides a better diameter resolution for particles in the micrometer and submicrometer region. A further advantage results from the alternating part of the scattered power of a reference system which is given by the product of the field strengths of the reference and scattered wave instead of two scattered waves. As a consequence, the decrease of the alternating signal amplitude with the particle diameter in Fig. 7 is much smaller (in the Rayleigh region: $P_{AC} \sim d_p^3$ instead of d_p^6). Hence, with a reference beam PDA based on low-noise lasers (laser diodes, Nd:YAG lasers), particle sizing in the submicrometer range can be realized with relatively modest efforts.

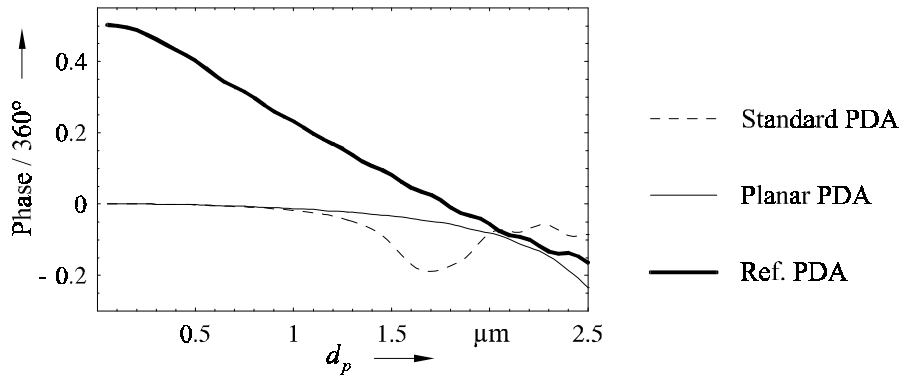

Fig. 6: Phase difference as a function of the particle diameter for a standard PDA ($\varphi = 30°$, $\psi = \pm 20°$), planar PDA ($\varphi = 0°, \psi = \pm 20°$) and reference beam PDA (m = 1.33, λ = 852 nm, $\theta = 9°$)

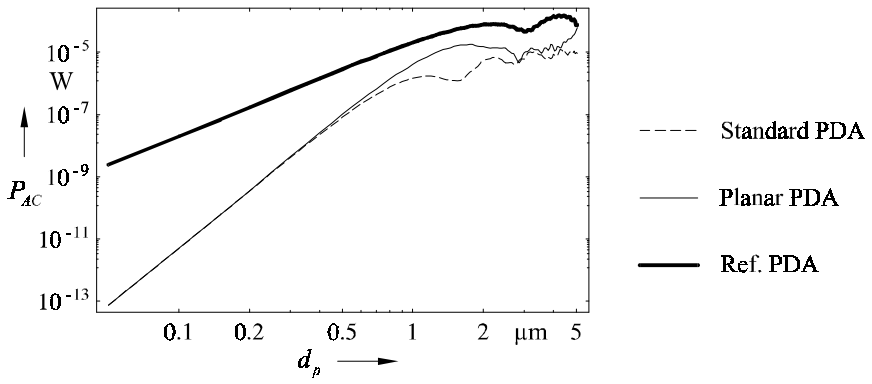

Fig. 7: Alternating part of the light power on the receiver as a function of the particle diameter (Parameters: $m = 1.33$, $\lambda = 852$ nm, $\theta = 9°$) for a standard PDA ($\varphi = 30°$, $\psi = \pm 20°$, $NA = 0.05$), planar PDA ($\varphi = 0°$, $\psi = \pm 20°$, $NA = 0.05$) and reference beam PDA ($NA = 7.1 \times 10^{-4}$)

3. SIGNAL PROCESSING

The alternating part of a measured Doppler signal can be described by the equation

$$\mathrm{f}(t) = A\,\mathrm{e}^{-2\frac{(t-t_{\max})^2}{t_B^2}}\cos(\omega_D t - \phi) \tag{20}$$

with the signal amplitude A, the time of the signal maximum $t_{\max}$, the half burst duration t_B, the angular frequency $\omega_D = 2\pi f_D$ and phase ϕ (Fig. 8a). A location of the particle trajectory inside the measurement volume and simultaneous particle sizing based on the methods given in section 2 require an estimation of the Doppler frequency, the time displacement and the phase difference of the Doppler signals. Especially for Doppler signals with low signal-to-noise ratios, signal processing in the frequency domain is advantageous and quite usual. The Fourier transform of the function $\mathrm{f}(t)$ according to Eq. (20) is given by

$$\mathrm{F}\{\mathrm{f}(t)\} = \frac{A}{2}\sqrt{\frac{\pi}{2}}\,t_B\left(\mathrm{e}^{-\frac{t_B^2(\omega+\omega_D)^2}{8} - j((\omega+\omega_D)\,t_{\max}-\phi)} + \mathrm{e}^{-\frac{t_B^2(\omega-\omega_D)^2}{8} + j((\omega-\omega_D)\,t_{\max}-\phi)}\right). \tag{21}$$

An efficient discrete computation of the Fourier transform of digitized samples can be performed by the well-known fast Fourier transform (FFT). The highest spectral line in the discrete amplitude spectrum is only a first approximation to the Doppler frequency f_D (Fig. 8b). Several interpolation procedures have been developed to improve the accuracy of the frequency estimation (Shinpaugh et al. 1992), e. g. centroid, parabolic and Gaussian fits. The latter is especially suited for Doppler signals with a Gaussian envelope and a burst duration smaller than the sampled time window (essential for the described time displacement method). A more recent analysis which is quite efficient even for Doppler signals truncated by the sampled time window is similar to the centroid fit but uses a weighted evaluation scheme of the center of gravity of the complete Doppler peak. With squared amplitudes of the spectral lines $a^2(i)$ at the discrete frequencies *i*, the weighting coefficients $g(i)$ and the integer number *n* of f_D, the Doppler frequency is given by

$$f_D = \sum_{i=n-\#}^{i=n+\#} g(i)\,a^2(i)\,i \Bigg/ \sum_{i=n-\#}^{i=n+\#} g(i)\,a^2(i)\,. \tag{22}$$

In a first step the weighting coefficients are 1 but the coefficients at $i = n \pm \#$ are only $1/2$. This equation is iterated up to the case that the integer number *n* of f_D remains unchanged. Then the weighting coefficients at the boundaries are replaced by

$$g(i = n-\#) = 1/2 + (n - f_D) \quad \text{and} \quad g(i = n+\#) = 1/2 - (n - f_D) \tag{23}$$

and the remaining quadratic expression for f_D then is solved. The value # is dependent on the number of fringes in the measurement volume and on the sampled window in the time domain of the digitizer. Usually it can be set to 3 or 4 and may be increased with rising frequency. This procedure is reliable to obtain a center of gravity in the middle of the examined peak area with linearly interpolated edges and to avoid digitizing artifacts. Secondly, the routine is faster than transcendental functions, e. g. interpolation by trigonometric or logarithmic algorithms.

The estimation of the phase difference of the Doppler signals is well known from signal processing algorithms used in the phase Doppler technique. According to Eq. (21), the phase spectrum of a Doppler signal $\mathrm{Arg}[\mathrm{F}\{\mathrm{f}(t)\}]$ shows a linear behavior around the Doppler frequency. A linear fit of the phase values at the Doppler frequency gives the phase ϕ of the Gaussian modulated harmonic $\mathrm{f}(t)$. The phase difference at the Doppler frequency can be taken as the difference of both phase spectra or from the phase of the cross-correlation function (CCF) as described by Domnick et al. (1988).

A rather exceptional case in the laser Doppler and phase Doppler technique is the estimation of the time of the signal maximum $t_{\max}$ and the time displacement between two Doppler signals $\Delta t_{12} = t_{\max 1} - t_{\max 2}$, respectively. Considering the Fourier transform of a Doppler signal $\mathrm{F}\{\mathrm{f}(t)\}$ according to Eq. (21), the time of the signal maximum $t_{\max}$ is given by the linear gradient in the phase spectrum

$$t_{\max} = \frac{1}{2\pi} \frac{\mathrm{d}\,\phi(f)}{\mathrm{d}\,f} \quad , \tag{24}$$

which can be calculated according to the linear fit already used for the estimation of the signal phase. Similar to the phase difference, the time displacement between two Doppler signals can be calculated from two phase gradients of the two phase spectra or from one phase gradient in the phase spectrum of the CCF (Albrecht et al. 1993). To use to the farthest possible extent spectral lines above the noise floor in the spectrum, the 2π ambiguities of the phase have to be eliminated. Since the time of the signal maximum $t_{\max}$ has to be after the first sample, this can be achieved by allowing only positive phase gradients in the phase spectrum of one Doppler signal (Fig. 8c,d). The phase gradient in the CCF can be positive or negative. Therefore an elimination of the 2π ambiguities is possible only on condition that the absolute value of the time displacement between the two Doppler signals is smaller than half the length of the sampled time window (Borys 1996).

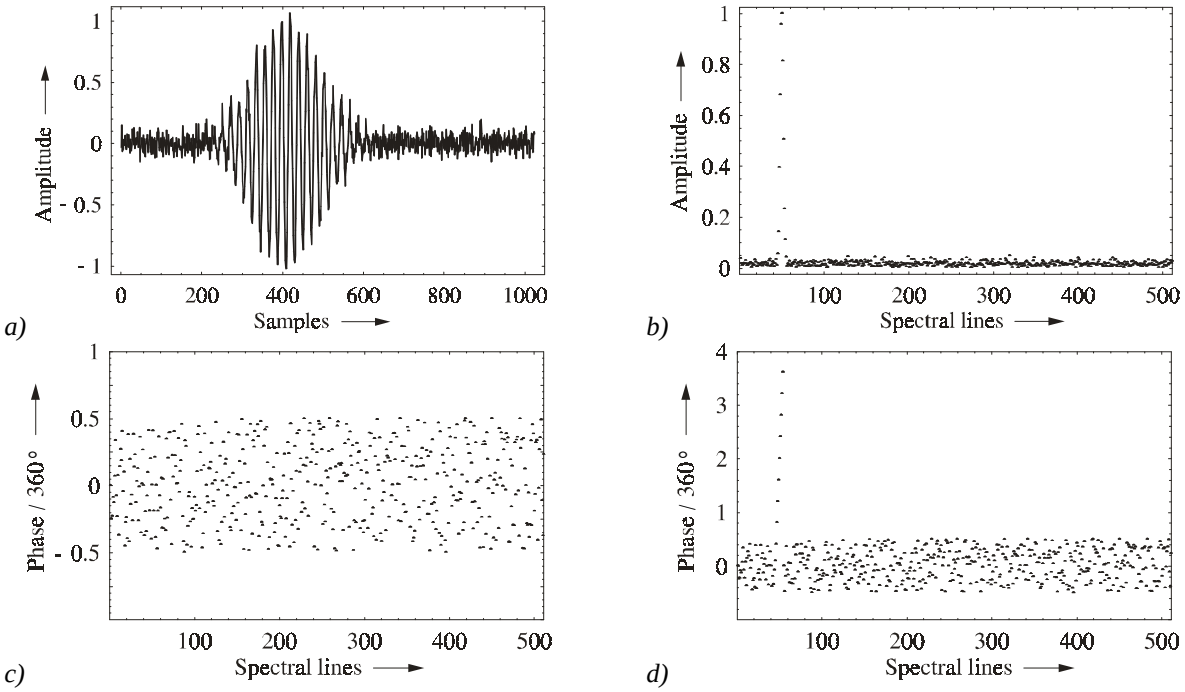

Fig. 8: a) Alternating part of the received Doppler signal, b) Amplitude spectrum, c) Phase spectrum, d) Phase spectrum with eliminated 2π ambiguities

3. EXPERIMENTAL VERIFICATION

To verify the fundamentals of the described measuring techniques, different experimental investigations had to be carried out. First we proved the time displacement and the phase difference method to locate the particle trajectory. For the receivers R_1 and R_3 in Fig. 1, an integrated two-element PIN diode with a diameter of the sensitive surfaces of $d_r = 500$ µm and a displacement of their centers in the x-direction of $x_r = 550$ µm (CENTRONIC Ltd., type LD2-5T) was applied. For the receiver R_2 in Fig. 1, we used a normal PIN diode. With both systems the position of a wire with a diameter of 25 µm was measured. The wire was fixed on a rotating disk and traversed through the measurement volume. Figure 9a gives an example of the resolution

obtained by a relative displacement of the wire in steps of 20 µm over a length of 200 µm. Because of the longer time window, which has to be sampled for the time displacement method in order to cover the displaced Doppler signals without a significant truncation, the average SNR was about 5 dB lower than the SNR of the signals sampled for the phase difference method (23 dB). For the standard deviation of the measured coordinates by the time displacement method we obtained values between 12 µm and 16 µm and for the phase difference method between 7 µm and 9 µm. The average deviation of the mean values of both methods was significantly smaller than 10 µm. Additionally coincident measurements were performed with both systems in front of a wind tunnel nozzle. Figure 9b shows the good correlation between the raw data measured over a length of approximately 8 mm by the time displacement and the phase difference method.

In the experiments for simultaneous particle sizing, in addition to the reference beam PDA, a planar PDA and a common seeding generator (DANTEC, type 55L18) were used. A preliminary examination of the size distribution of this seeding generator gives a mean geometric droplet diameter of 1.65 µm with a standard deviation of 0.3 µm.

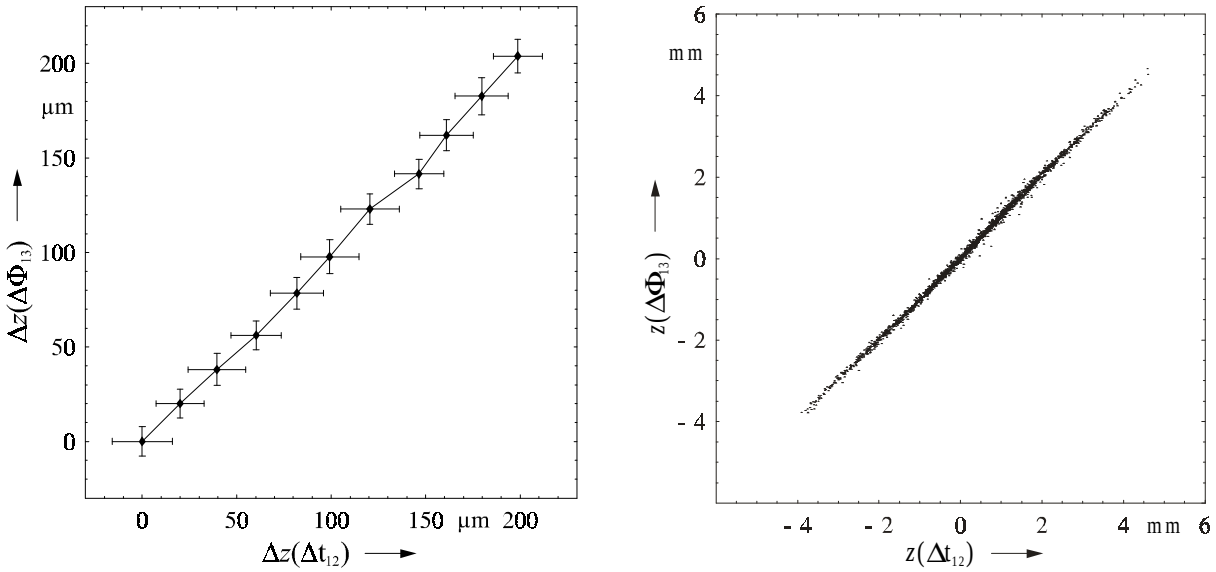

a) b)

Fig. 9: a) Comparison between time displacement and phase difference method for a location of the position of a wire (diameter 25 µm) in the measurement volume, b) correlation of coincident measurements with both systems in front of a wind tunnel nozzle

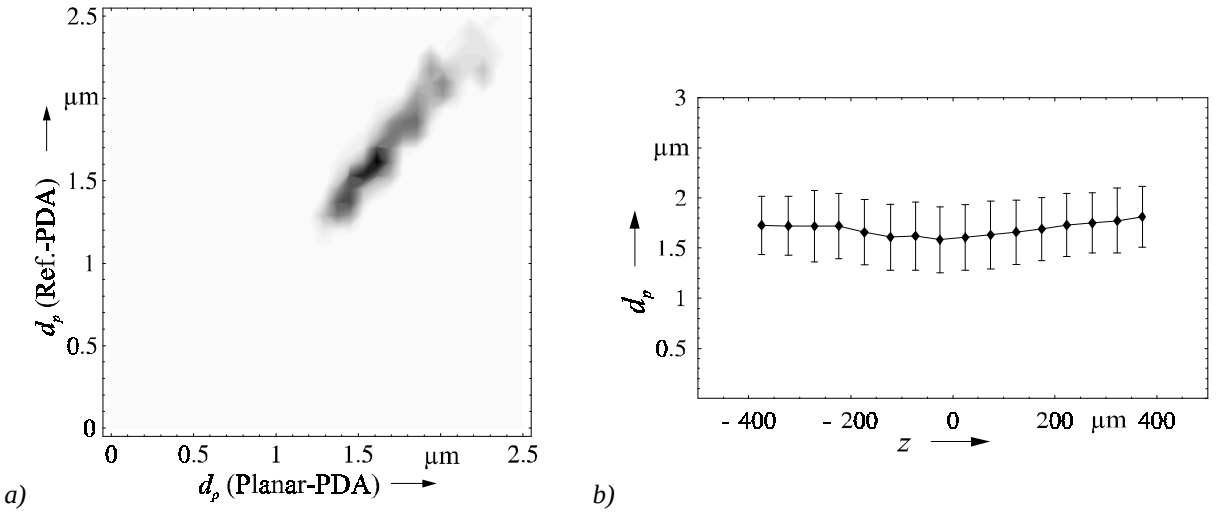

a) b)

Fig. 10: Coincident measurements with planar and reference beam PDA: a) correlation of measured particle sizes, b) measured particle sizes as a function of the z-coordinate inside the measurement volume of the planar PDA ($m = 1.33$, $\lambda = 852$ nm, $\theta = 9°$, Planar-PDA: $\psi = \pm 11.5°$)

Figure 10 shows the results of a coincident measurement with a planar and a reference beam system in a free flow of the seeding generator. Since the signal rate of the reference system was much higher, it was triggered by the planar PDA for coincident measurements. The measured diameters of both systems are in compliance with each other. Because of the poor sensitivity of the planar system for particles smaller 1.2 µm, the size distribution is truncated towards smaller particles. With the coincident measurements the measured particle sizes can be resolved inside the measurement volume of the planar system by evaluating the time shift of the reference signals according to Eq. (1). As a result of the higher light intensity, Fig. 10b shows a minor shift towards smaller particles in the center of the measurement volume of the planar system. In order to change the spatial size distribution, a plane glass plate was placed in the free flow of the seeding generator. Figure 11 shows the profiles of the velocity and particle sizes in the boundary layer measured with the reference PDA. In spite of the low velocity gradient and the narrow particle size distribution of the seeding generator (σ = 0.3 µm), the dependence of the detected particle sizes on the distance from the surface of the glass plate is obvious.

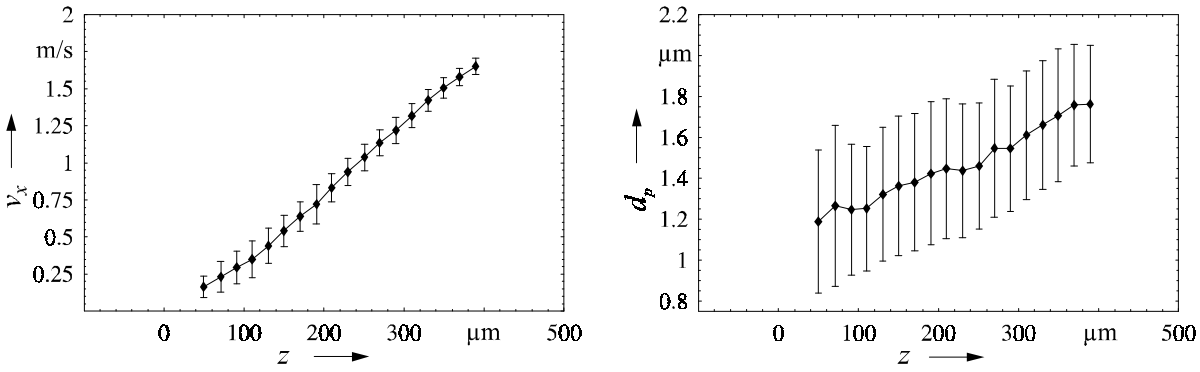

a) *b)*

Fig. 11: Local dependencies of the velocity (a) and detected particle sizes (b) in a boundary layer of a plane plate in a free flow of a seeding generator measured with the reference beam PDA (z-coordinate perpendicular to the surface of the plate with respect to the center of the measurement volume)

3. SUMMARY AND CONCLUSIONS

Two alternative methods to locate the particle trajectory in the measurement volume of a reference beam arrangement have been described and experimentally verified. Both methods enable an estimation of the particle trajectory in the plane of the laser beams over a length of about 10 mm. The resolution depends on the measurement range and the signal quality. Since the phase difference method according to Eq. (6) projects the measured length onto a phase range of 2π and a phase resolution of about one degree can be achieved for good SNR values of about 15 dB and 512 sample points (Domnick et al. 1988, Ibrahim et al. 1991), a resolution of less than 0.3% of the measurement range seems to be achievable. Because of the dependence of the measurement range on the receiver aperture, i. e. receiver distance and diameter, a length of e. g. 1 cm or only 1 mm can be measured with an estimated resolution of about 30 µm and 3 µm, respectively. This offers the possibility of adapting the measurement range and resolution to the application. If a shifted optical system is used even the *z*-coordinate of scatterers without a velocity component in x-direction can be measured by the phase difference method.

Furthermore, theory and first results of a phase Doppler system based on the reference beam technique have been presented. The new method allows the simultaneous measurement of velocity, size and position of the scattering particle inside the measurement volume with a spatial resolution in the order of magnitude of 10 µm. The reference beam PDA is advantageous for the measurement of particles in the size range below 3 µm. It allows simultaneous measurement of velocity and particle size profiles in boundary layers and can be used in extension of common phase Doppler systems to generally improve the spatial and size resolution.

REFERENCES

Albrecht, H.-E.: Laser-Doppler-Strömungsmessung. Akademie-Verlag, Berlin 1986

Albrecht, H.-E.; Borys, M.; Hübner, K. (1993): Generalized theory for the simultaneous measurement of particle size and velocity using laser Doppler and laser two-focus methods. Part. Part. Syst. Charact. 10, pp. 138–145

Albrecht, H.-E.; Bech, H.; Damaschke, N.; Feleke, M. (1995): Berechnung der Streuintensität eines beliebig im Laserstrahl positionierten Teilchens mit Hilfe der zweidimensionalen Fouriertransformation. Optik 100, S. 118–124

Bachalo, W. D.; Houser, M. J. (1984): Phase-Doppler-spray analyzer for simultaneous measurements of drop size and velocity distributions. Opt. Engineering 23, pp. 583-590

Bauckhage, K.; Flögel, H.-H. (1984): Correlation of simultaneously measured droplet sizes and velocities in nozzle sprays. Part. & Part. Syst. Charact. 1, pp. 112-116

Borys, M. (1996): Analyse des Amplituden- und Phasenverhaltens von Laser-Doppler-Signalen zur Größenbestimmung sphärischer Teilchen. Universität Rostock, Dissertation 1996, Zugl.: Shaker Verlag, Aachen 1996

Borys, M.; Strunck, V.; Müller, H.; Dopheide D. (1998): Meßvolumeneffekte des Referenzstrahl-LDAs. In: Lasermethoden in der Strömungsmeßtechnik, 6. Fachtagung der Deutschen Gesellschaft für Laser-Anemometrie GALA, Essen, Verlag Shaker, Aachen, S. 38.1–38.6

Chalé-Góngora, H. G.; Brun, M. (1998): Application of two-component phase Doppler anemometry to the study of transient diesel spray impingement. Proc. 9th Int. Symp. on Applications of Laser Techniques to Fluid Mechanics, Lisbon, pp. 7.5.1–7.5.8

Compton, D. A.; Eaton J. K. (1996): A high-resolution laser Doppler anemometer for three-dimensional turbulent boundary layers. Exp. in Fluids 22, pp. 111–117

Desantes, J. M.; Arrégle, J.; Pastor, J. V.; González, U. (1998): Diesel spray wall impingement characterisation by means of PDA and high speed visualisation. Proc. 9th Int. Symp. on Applications of Laser Techniques to Fluid Mechanics, Lisbon, pp. 7.6.1–7.6.8

Domnick, J.; Ertel, H.; Tropea, C. (1988): Processing of phase Doppler signals using cross spectral density function. In: Selected papers of the 4th Int. Symp. on Appl. of Laser Anemometry to Fluid Mechanics, Lisbon, Springer Verlag, Berlin, pp. 473–483

Dopheide, D.; Strunck, V.; Krey, E.-A. (1993): Three component laser Doppler anemometer for gas flowrate measurements up to 5500 m³/h. Metrologia 30, pp. 453–469

Drain, L. E. (1980): The laser Doppler technique. John Wiley & Sons, New York

Durst, F.; Kikura, H.; Lekakis, I.; Jovanovic, J.; Ye, Q. (1996): Wall shear stress determination from near-wall mean velocity data in turbulent pipe and channel flows. Exp. in Fluids 20, pp. 417–428

Gusmeroli, V.; Martinelli, M. (1991): Distributed laser Doppler velocimeter. Optics Letters 16, pp. 1358–1360

Ibrahim, K. M.; Wertheimer, G. D.; Bachalo, W. D. (1991): Signal processing considerations for low signal to noise ratio laser Doppler and phase Doppler signals. Proc. 4th Int. Conf. on Laser Anemometry, Advances and Applications, Ohio, pp. 685–692

Karlson, R. I.; Eriksson, J.; Persson, J. (1992): LDV measurements in a plane wall jet in a large enclosure. Proc. 6th Int. Symp. on Appl. of Laser Techniques to Fluid Mechanics, Lisbon, pp. 1.5.1–1.5.6

Mazumder, M. K.; Wanchoo, S.; McLeod, P. C.; Ballard, G. S.; Mozumdar, S.; Caraballo, N. (1981): Skin friction drag measurements by LDV. Appl. Opt. 20, pp. 2832–2837

Saffman, M.; Buchhave, H.; Tanger, H. (1984): Simultaneous measurement of size, concentration and velocity of spherical particles by a laser Doppler anemometer method. Proc. 2nd Int. Symp. on Application of Laser Anemometry to Fluid Mechanics. Lisbon, pp. 8.1.1–8.1.6

Shinpaugh, K. A.; Simpson, R. L.; Wicks, A. L.; Ha, S. M.; Fleming, J. L. (1992): Signal processing techniques for low signal-to-noise ratio Doppler velocimetry signals. Experiments in Fluids 12, pp. 319–328

Strunck, V.; Grosche, G.; Dopheide, D. (1993): New laser Doppler sensors for spatial velocity information. Proc. Int. Congress on Instrumentation in Aerospace Simulation Facilities ICIASF'93, French-German Research Institute (ISL) Saint-Louis France, IEEE-Publication 93CH3199-7, pp. 36.1–36.5

Strunck, V.; Grosche, G.; Dopheide, D. (1994): Scanning laser-Doppler probe for profile measurements. Proc. 7th Int. Symp. on Applications of Laser Techniques to Fluid Mechanics, Lisbon, pp. 17.1.1–17.1.5

Strunck, V.; Müller, H.; Dopheide, D. (1998): Traversionsfreie LDA-Grenzschichtmessungen mit Mikrometerauflösung im Meßvolumen. In: Lasermethoden in der Strömungsmeßtechnik, 6. Fachtagung der Deutschen Gesellschaft für Laser-Anemometrie GALA, Essen, Verlag Shaker, Aachen, S. 28.1–28.11

Taniere, A.; Boulet, P.; Oesterle, B. (1997): Analysis of laser Doppler anemometer measurements: Saltation effects in the behaviour of solid particles. Proc. 7th Int. Conf. Laser Anemometry Advances and Applications, Karlsruhe, pp. 737–744

Wei, T.; Willmarth, W. W. (1989): Reynolds-number effects on the structure of a turbulent flow. J. Fluid Mech. 204, pp. 57–95

Wittig, S.; Elsäßer, A.; Samenfink, W.; Ebner, J.; Dullenkopf, K. (1996): Velocity profiles in shear-driven liquid films: LDV-measurements. 8th Int. Symp. on Applications of Laser Techniques to Fluid Mechanics, Lisbon, pp. 25.2.1–25.2.8

Yeh, Y.; Cummins, H. Z.: Localized fluid flow measurements with a He-Ne laser spectrometer. Appl. Phys. Lett., Vol. 4 (1964), pp. 176-178